COMPARISON OF GLOBAL GEOPOTENTIAL MODELS FROM THE CHAMP AND GRACE MISSIONS FOR REGIONAL GEOID MODELLING IN TURKEY

BIHTER EROL[1], MICHAEL G. SIDERIS[2] AND RAHMI N. ÇELIK[1]

1 Department of Geodesy and Photogrammetry Engineering, Istanbul Technical University, Civil Engineering Faculty, Maslak, 34469, Istanbul, Turkey (bihter@itu.edu.tr, celikn@itu.edu.tr)

2 Department of Geomatics Engineering, University of Calgary, 2500 University Drive N.W., Calgary, Alberta T2N 1N4, Canada (sideris@ucalgary.ca)

Received: June 4, 2008; Revised: October 20, 2008; Accepted: May 27, 2009

ABSTRACT

The continuous efforts on establishment and modernization of the geodetic control in Turkey include a number of regional geoid models that have been determined since 1976. The recently released gravimetric Geoid of Turkey, TG03, is used in geodetic applications where GPS-heights need to be converted to the local vertical datum. To reach a regional geoid model with improved accuracy, the selection of the appropriate global geopotential model is of primary importance. This study assesses the performance of a number of recent satellite-only and combined global geopotential models (GGMs) derived from CHAMP and GRACE missions' data in comparison to the older EGM96 model, which is the underlying reference model for TG03. In this respect, gravity anomalies and geoid heights from the global geopotential models were compared with terrestrial gravity data and low-pass filtered GPS/levelling data, respectively. Also, five new gravimetric geoid models, computed by the Fast Fourier Transform technique using terrestrial gravity data and the geopotential models, were validated at the GPS/levelling benchmarks. The findings were also compared with the validation results of the TG03 model.

The tests showed that as it was expected any of the high-degree combined models (EIGEN-CG03C, EIGEN-GL04C, EGM96) can be employed for determining the gravity anomalies over Turkey. In the west of Turkey, EGM96 and EIGEN-CHAMP03S fit the GPS/levelling surface better. However, all the tested GGMs revealed equal performance when they were employed in gravimetric geoid modelling after de-trending the gravimetric geoid model with corrector surface fitting. The new geoid models have improved accuracy (after fit) compared to TG03.

Key words: Global Geopotential Models, CHAMP, GRACE, GPS/levelling, filtering, gravity anomalies, Remove-Compute-Restore method

1. INTRODUCTION

In geodetic applications, there is a growing need for knowledge of the regional geoid surface with high accuracy to transform GPS-derived heights to the regional vertical datum. The recently released Geoid of Turkey TG03, which is a gravimetric geoid model fitted to the regional vertical datum using GPS/levelling data, has an absolute accuracy of around 15 cm (*Erol, 2007*; *TNGC, 2003*). Our studies on the determination of a geoid surface with improved accuracy in the region are part of the modernizing effort of the vertical control in Turkey.

Recent developments in satellite techniques and computation algorithms promise further improvements in the determination of the global gravity field models. With the launch of the CHAMP (CHAllenging Minisatellite Payload) and GRACE (Gravity Recovery and Climate Experiment) satellite gravity missions, whose data have led to the computation of a number of global geopotential models (GGMs), improvement in the long and medium wavelengths of the gravity field spectrum (up to degree 120) have been achieved (*Förste et al., 2006*; *NIMA, 1997*; *Reigber et al., 2004*; *Tapley et al., 2005*), and hence corresponding improvements are expected for regional geoid models, as well. This is because precise regional geoid model determination typically includes a GGM as underlying geopotential representation together with a set of point or mean terrestrial gravity data and topographic information.

With this expectation, a number of recent CHAMP- and GRACE-derived GGMs are assessed in the context of forming an appropriate base for an improved regional geoid model in Turkey. In order to determine a suitable GGM as the base model, a comparison and validation of the GGMs with independent geoid and gravity information, such as GPS/levelling heights and gravity anomalies is needed (*Gruber, 2004*; *Kiamehr and Sjöberg, 2005*; *Merry, 2007*). Therefore, firstly, the statistical fit of the candidate GGMs, namely GGM02S, EIGEN-CHAMP03S, EIGEN-CG03C and EIGEN-GL04C, to the gravity field in Turkey was investigated. These models were also compared with the EGM96 model, which was one of the most complete and accurate GGMs until recently (*Smith, 1998*; *Kiamehr and Sjöberg, 2005*; *Merry, 2007*) and which serves as the underlying model for TG03.

In the numerical evaluations, GGM-based gravity anomalies were computed and compared with a grid of terrestrial gravity anomalies over the whole country to assess the fit of each GGM to the gravity field of Turkey. In addition, the GGM-derived geoid heights were also compared with the filtered GPS/levelling geoid heights in western Turkey. The numerical tests were done in the Istanbul-1999 and Izmir-2001 local GPS/levelling networks, which are in the north-western and western parts of Turkey, respectively. The GPS/levelling benchmarks of both networks were established appropriately to characterize the changes of the topography well, and are densely and homogeneously distributed over the area. The GPS and levelling data of the networks, which fulfil the criteria put forth by the current Large Scale Map and Spatial Data Production Regulation of Turkey, are accurate enough for geoid modelling and testing (*Deniz et al., 2008*).

The GGMs were evaluated in gravimetric geoid modelling using Stokes's method, where they were employed as the reference models for computing five new gravimetric

geoid models by the Remove-Compute-Restore (RCR) technique. In these computations, a grid of terrestrial gravity anomalies on land and satellite altimetry derived gravity anomalies at sea were employed. Shuttle Radar Topography Mission (SRTM) data were used to compute the topographic effects. The new gravimetric geoids were also fitted to the regional vertical datum using GPS/levelling data, and statistics were produced of the geoid height discrepancies at the independent GPS/levelling benchmarks. In addition, the validation results of the fitted geoid models against local GPS/levelling data were also compared with the validation results of TG03.

2. GLOBAL GEOPOTENTIAL MODELS AND DATA USED

Earth geopotential models can be divided into three classes based on the data used in their computation, namely *satellite-only GGMs* (derived from the tracking of artificial satellites), *combined GGMs* (derived from the combination of a satellite-only model with terrestrial and/or airborne gravimetry, satellite altimetry, and topography/bathymetry) and *tailored GGMs* (derived by refining existing satellite-only or combined GGMs using regional gravity and topography data).

Satellite-only GGMs are typically weak at coefficients of degrees higher than 60 or 70 due to several factors, such as the power-decay of the gravitational field with altitude, modelling of atmospheric drag, incomplete tracking of satellite orbits from the ground stations etc. (*Rummel et al., 2002*). Although the effects of some of these limitations on the GGMs decreased after the dedicated satellite gravity missions CHAMP and GRACE (*GGM02, 2004*; *GFZ, 2006*), the new satellite-only GGMs still have full power until a certain degree, and rapidly increasing errors make their coefficients unreliable at high degrees see, e.g., Fig. 1 (*Tapley et al., 2005*; *ICGEM, 2005*). On the other hand, the combined-GGMs reduce some of the aforementioned limitations, but the errors in the terrestrial data remain.

In this study, recent satellite-only and combined GGMs from the CHAMP and GRACE satellite missions released by GeoForschungsZentrum (GFZ) in Germany and the Center for Space Research (CSR) of the University of Texas at Austin were tested.

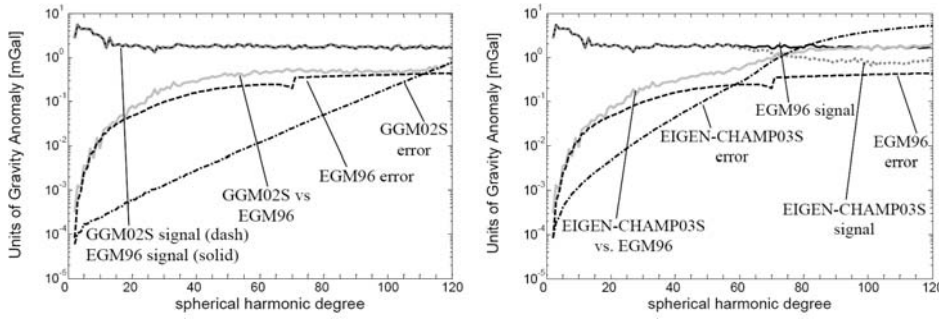

Fig. 1. The power spectrums of the GGM02S and the EIGEN-CHAMP03S models versus EGM96 model, respectively (in mGal) (*Erol, 2007*).

Table 1. List of the global geopotential models which are assessed in the numerical tests.

Model*	Degree	Type	Tide System**	Citation
GGM02S	160	satellite-only	zero-tide	*Tapley et al. (2005)*
EIGEN-CHAMP03S	140	satellite-only	tide-free	*Reigber et al. (2004)*
EGM96	360	combined	tide-free	*Lemoine et al. (1998)*
EIGEN-CG03C	360	combined	tide-free	*Förste et al. (2005)*
EIGEN-GL04C	360	combined	tide-free	*Förste et al. (2006)*

* the coefficients of the models are available from *ICGEM (2005)*.

** the GGM02S model has been converted to the tide-free system by applying correction to the coefficient C_{20}.

Table 1 summarizes the characteristics of these models. Although the older EGM96 combined geopotential model does not involve data from the CHAMP and GRACE missions, the study includes this model as well since it is the underlying model of TG03.

2.1. GGM02S

The GGM02S satellite-only geopotential model was computed using approximately 14 months of data (spanning from April 2002 to December 2003) of the GRACE K-band range-rate and accelerometer data (*Tapley et al., 2005*). The model was estimated to degree and order 160. However, the solution appears to retain the correct signal power spectrum up to about degree 110 (see Fig. 1 for the power spectrum of GGM02S in terms of gravity anomalies). Therefore its spherical harmonic coefficients were employed in this study up to maximum degree and order 110. Relative to its preceding release GGM01S, an improvement greater than a factor of two is reported by *Tapley et al. (2005*).

2.2. EIGEN-CHAMP03S

EIGEN-CHAMP03S is a satellite-only geopotential model, which was derived using 33 months (from October 2000 through June 2003) of CHAMP data. The model contains fully normalized spherical harmonic coefficients complete to degree and order 120, plus selected terms for CHAMP sensitive and resonant orders up to degree 140. Although the EIGEN-CHAMP03S solution includes higher degree/order terms, it has full power only up to about degree and order 60 due to signal attenuation at satellite altitude (see Fig. 1 for the power spectrum of the model in terms of gravity anomalies) (*GFZ, 2006*). Therefore, the spherical harmonic coefficients of EIGEN-CHAMP03S were employed in this study up to maximum degree and order 60. The accuracy of EIGEN-CHAMP03S is reported to be about 5 cm and 0.5 mGal in terms of geoid heights and gravity anomalies, respectively, at half wavelengths of 400 km (*Reigber et al., 2004*).

2.3. EGM96

EGM96 is a combined geopotential model consisting of the spherical harmonic coefficients complete to degree and order 360. The National Imagery and Mapping Agency (NIMA), the NASA Goddard Space Flight Center (GSFC), and the Ohio State

University (OSU) collaborated in the determination of EGM96 model. The geoid accuracy of the model is better than one meter with the exception of areas void of dense and accurate surface gravity data (*Lemoine et al., 1998*; *Smith, 1998*; *EGM96, 2004*).

2.4. EIGEN-CG03C

The EIGEN-CG03C is a combined model, which was computed by the combination of GRACE mission data (376 days comprising the periods February to May 2003, July to December 2003 and February to July 2004), CHAMP mission data (period of 860 days from October to June 2003), and altimetric and gravimetric surface data available at GFZ Potsdam. The model is complete to degree and order 360. Compared to preceding CHAMP/GRACE combined high-resolution global geopotential models, *Förste et al. (2005)* reported an estimated improvement of one order of magnitude in accuracy (up to 3 cm and 0.4 mGal in terms of geoid heights and gravity anomalies, respectively, at a spatial resolution of 400 km). The overall accuracy of the full model is reported to be 30 cm and 8 mGal, in geoid heights and gravity anomalies, respectively.

2.5. EIGEN-GL04C

The EIGEN-GL04C combined model is an upgrade of the preceding EIGEN models and was computed with a combination of GRACE (from February 2003 to July 2005, excluding January 2005) and LAGEOS (for February 2003 to February 2005) mission data, combined with $30' \times 30'$ gravimetry and altimetry surface data provided by GFZ Potsdam and the Groupe de Recherche de Gèodésie Spatiale (GRGS) Toulouse. EIGEN-GL04C is complete to degree and order 360 (*Förste et al., 2006*; *Förste et al., 2008*). For more details of the GGMs, the references in Table 1 can be consulted.

2.6. Data Used

As mentioned before, in the first approach of testing the GGMs terrestrial gravity anomalies and GPS/levelling data were used. In the second approach of the tests, gravimetric geoid models were computed with the RCR technique, where satellite altimetry derived and terrestrial gravity anomalies as well as digital elevation models from different sources were employed. GPS/levelling data were again used to fit and to validate the gravimetric geoid models. Finally, the geoid models after fit were also compared to TG03 data.

The free-air gravity anomalies on land were restored from the regularly gridded Bouguer gravity anomalies (in 5'x5' spatial resolution) using the heights from ETOPO5 (*NOAA, 2005*). Then the free-air gravity anomalies on land and satellite altimetry derived gravity anomalies at sea were merged using a nearest-neighbourhood interpolation approach (see Fig. 2). The altimetric gravity anomalies were extracted from the KMS2002 data (in $2' \times 2'$ spatial resolution) (*KMS, 2002*).

For testing the GGMs, GPS/levelling data in the local Istanbul-1999 and Izmir-2001 networks were employed as well. The testing networks comprised 451 (Istanbul-1999) and 309 (Izmir-2001) GPS/levelling benchmarks.

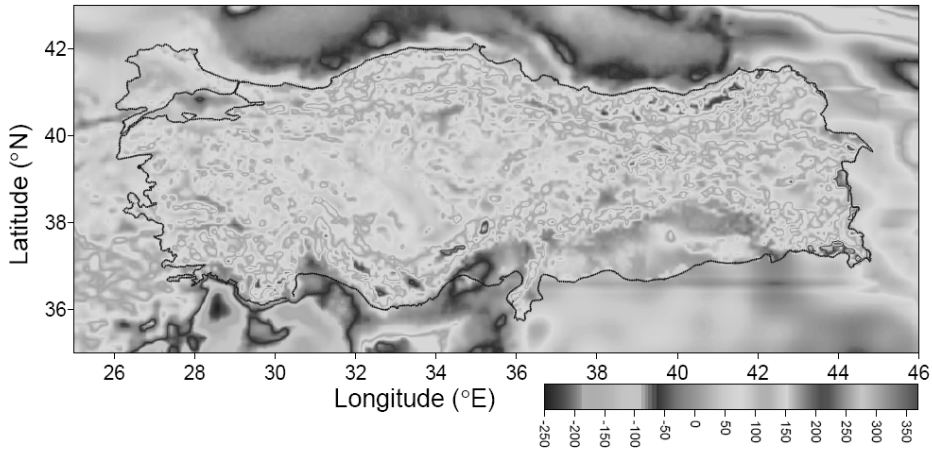

Fig. 2. Merged free-air gravity anomalies from terrestrial measurements on land (only inside of Turkey) and KMS02 satellite altimetry gravity anomalies at sea; units in mGal.

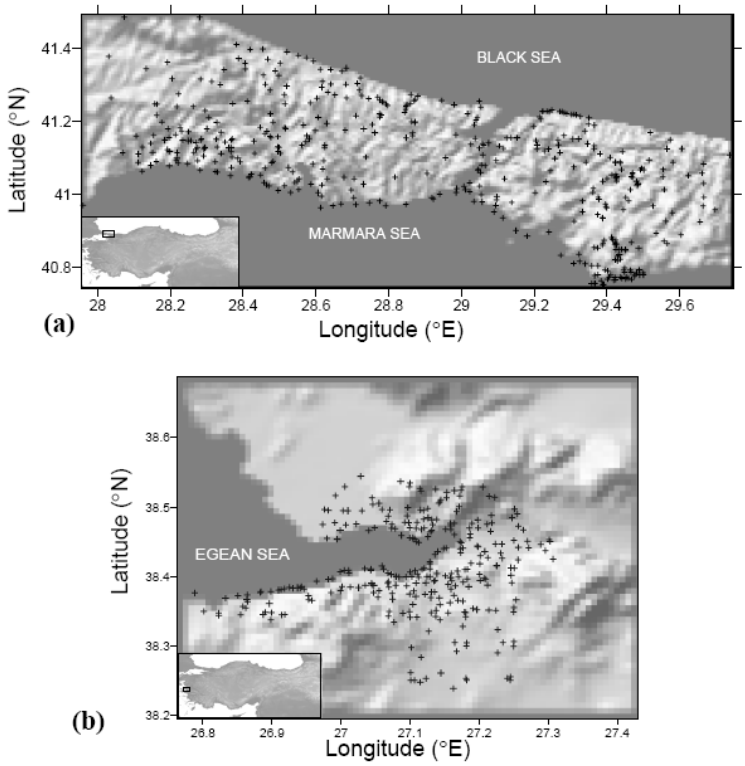

Fig. 3. Local GPS/levelling benchmarks: **(a)** Istanbul-1999, **(b)** Izmir-2001.

The Helmert orthometric heights of the benchmarks were determined by geometric levelling in Turkish National Vertical Datum (TUDKA99) and their absolute accuracy is 2.5 cm. GPS coordinates of the benchmarks refer to the ITRF96 datum. The accuracies of the GPS-derived coordinates are 1.5 cm and 2.3 cm in the horizontal and vertical directions (*Ayan et al., 1999*; *Ayan et al., 2001*). The Istanbul test area covers 65×160 km^2 and the Izmir test area covers 50×45 km^2. The densities of the benchmarks are approximately 1 benchmark per 23 km^2 in Istanbul and 1 benchmark per 8 km^2 in Izmir. The distributions of the benchmarks are shown in Fig. 3.

The outliers in the GPS/levelling data, caused by the errors in GPS and levelling observations, were detected considering geoid height differences at the benchmarks and eliminated. 11 benchmarks were removed from the Istanbul-1999 network and 8 from the Izmir-2001 network. Table 2 summarizes the properties of the data.

The topographical effects were considered using the Shuttle Radar Topography Mission (SRTM) derived digital elevation model. The SRTM data were produced from a collaborative mission by the National Aeronautics and Space Administration (NASA), the National Imagery and Mapping Agency (NIMA), the German Space Agency (DLR) and the Italian Space Agency (ASI) that generated a near-global digital elevation model of the Earth using Radar Interferometry (*EROS, 2002; Farr and Kobrick, 2000*). The unedited version of the SRTM data contains numerous occasional voids (areas without data) and gaps, especially in mountainous and coastline areas in western Turkey, therefore SRTM30 plus (in 30″ resolution) which is an enhanced form of the SRTM data using the GTOPO30 and digital depth model data *UCSD (2005)* was used. The SRTM heights are orthometric heights referenced to the EGM96 geoid (*NIMA, 1997; Lemoine et al., 1998*).

Table 2. Description of the local GPS/levelling networks.

	Description	Istanbul-1999	Izmir-2001
Network & Topography	Area [km^2]	75×200	56×45
	Number of GPS/levelling BMs*	450 (–7)	310 (–9)
	Density, 1 BM per km^2	1 / 32	1 / 8
	Elevation between [m]	1–585	1–1400
GPS Observations	GPS Receiver Type	dual frequency	dual frequency
	Number of Sessions & Duration	2 & 30 min	2 & 45 min
	Coordinate Datum	ITRF94	ITRF96
	2D Coordinate Accuracy [cm]	±1.0	±1.8
	h-Accuracy [cm]	±2.0	±2.5
Levelling	Levelling Method	geometric	geometric
	H-Accuracy [cm]	±2.0	±2.6
	Vertical Datum**	TUDKA99	TUDKA99
Geometry	Network Geometry	good	good
	Density of BMs	mixed	dense
	Distribution of BMs	non-homogenous	homogenous

* in parentheses: the number of benchmarks (BMs) removed as outliers.

** TUDKA99 is a Turkish National Control Network 1999 that provides Helmert Orthometric Heights.

In Turkey, various regional geoid models have been computed with different methods since 1970's (see *Ayan, 1976*; *Ayhan, 1993*; *Ayhan and Kilicoglu, 1993*; *TNFGN, 2002*; *TNGC, 2003*). In 2003, the General Command of Mapping released the most recent official regional gravimetric geoid model of Turkey, TG03. To compute TG03, the gravimetrically determined geoid model was fitted to the regional vertical datum at 197 GPS/levelling benchmarks, which are homogeneously distributed throughout the country (Fig. 4), by the *adjustable tension continuous curvature surface gridding algorithm* (*TNGC, 2003*). The long-wavelength part of this hybrid model is represented by the EGM96 geopotential model. The dense terrestrial gravity data of Turkey (with 3–5 km density, in modified Potsdam gravity datum) were employed together with marine gravity data and a terrain elevation model (450×450 m resolution) to calculate the short and medium wavelength components of the model. In *TNGC (2003)*, the absolute accuracy of TG03 is reported as 8.8 cm in the central territories and 20 cm along the coastlines and boundaries of the country. The TG03 data on a $3' \times 3'$ grid were used in the assessments.

Table 3 gives the basic statistics of the terrestrial data (free-air gravity anomalies, GPS/levelling and TG03 derived geoid heights) employed in the tests. These statistics show that the gravity field has more variable pattern in Istanbul than in Izmir and this information will be useful for interpretation of the test results later on.

3. NUMERICAL TESTS

In the initial assessments, the aforementioned GGMs in various degrees of the harmonic expansions were tested against terrestrial data, namely free-air gravity anomalies at grid nodes with 30′ resolution and local low-pass filtered GPS/levelling data at co-located benchmarks.

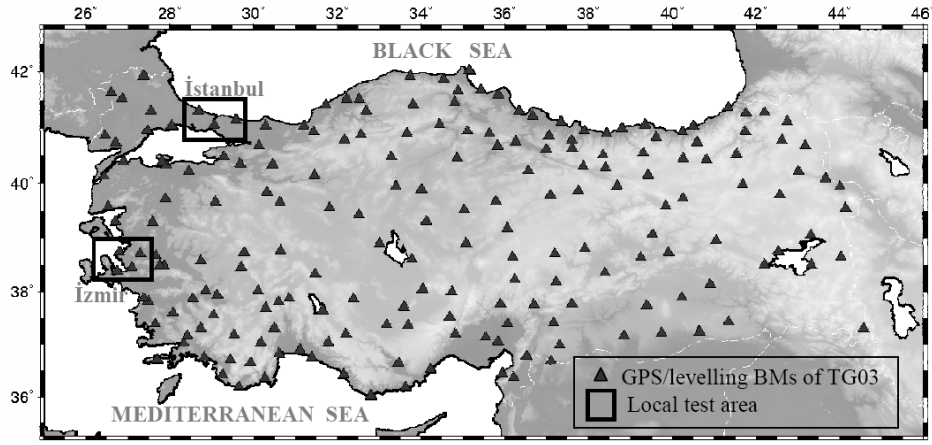

Fig. 4. 197 GPS/levelling benchmarks (BMs) employed in the computation of TG03 and locations of the test areas (*TNGC, 2003*).

Table 3. Comparison of the statistics of the terrestrial and TG03 data in local areas.

	Data	Min	Max	Mean	Std. Dev.
Istanbul	$\Delta g_{\text{Free-air}}$ [mGal]	−13.65	188.34	46.91	25.80
	$N_{\text{GPS/lev.}}$ [m]	35.83	38.23	36.95	0.45
	N_{TG03} [m]	35.77	38.12	36.92	0.42
Izmir	$\Delta g_{\text{Free-air}}$ [mGal]	−11.81	63.72	20.42	17.79
	$N_{\text{GPS/lev.}}$ [m]	37.59	38.73	38.06	0.16
	N_{TG03} [m]	37.60	38.40	38.01	0.13

The geoid height was determined from spherical harmonic coefficients $\bar{C}_{\ell m}$ and $\bar{S}_{\ell m}$. The infinite series was truncated at a maximum resolvable degree ℓ_{max}, corresponding to spatial-resolution $D = 20000/\ell_{max}$ (half wavelength given in km). The GGM derived geoid heights N_{GGM} can be obtained from

$$N_{GGM} \approx R \sum_{\ell=2}^{\ell_{max}} \sum_{m=0}^{\ell} \bar{P}_{\ell m}(\sin\theta)\left[\bar{C}_{\ell m}\cos m\lambda + \bar{S}_{\ell m}\sin m\lambda\right] \tag{1}$$

and the GGM-implied gravity anomaly is given by

$$\Delta g_{GGM} \approx \gamma \sum_{\ell=2}^{\ell_{max}} (\ell-1) \sum_{m=0}^{\ell} \bar{P}_{\ell m}(\sin\theta)\left[\bar{C}_{\ell m}\cos m\lambda + \bar{S}_{\ell m}\sin m\lambda\right], \tag{2}$$

where R is the mean radius of the Earth, (θ, λ) are co-latitude and longitude of the computation point, $\bar{P}_{\ell m}$ are fully normalized Legendre functions for degree ℓ and order m, $\bar{C}_{\ell m}$ and $\bar{S}_{\ell m}$ are fully normalized geopotential coefficients of the anomalous potential, γ is the mean gravity of the reference ellipsoid, and ℓ_{max} is the maximum degree of the GGM (*Heiskanen and Moritz, 1967*).

3.1. Filtering GPS/Levelling Data

In order to employ the low-frequency content of the GPS/levelling signal in the assessment of the GGM-derived geoid heights in local areas, the Discrete Meyer Wavelet Transform (DMWT) technique was applied. DMWT is a Discrete Wavelet Transform (DWT) which employs the Meyer function as the mother wavelet function (see Fig. 5). A wavelet frame, where the signal is completely represented by its spectrum, is formed by the scale (level) s and translation t parameters (see Fig. 6 and Eq.(3)).

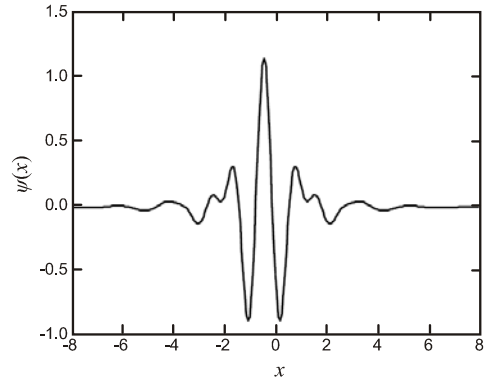

Fig. 5. Meyer Wavelet function $\psi(x)$.

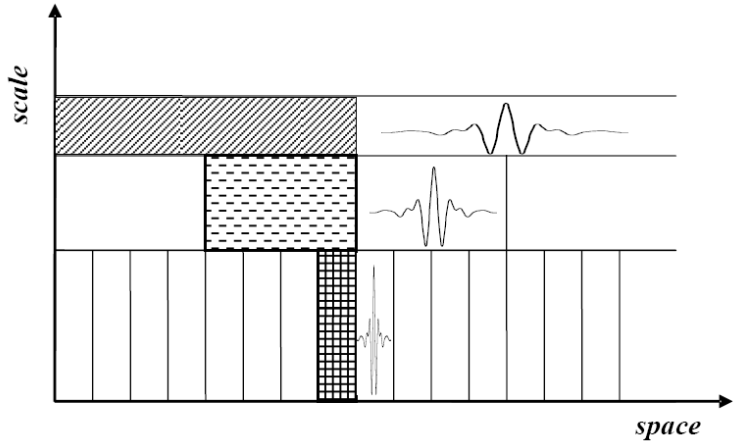

Fig. 6. The Meyer wavelet basis functions, space-scale tiles and coverage of the space-scale plane.

The filtering process in wavelet analysis is illustrated in Fig. 7. The original signal q passes through two complementary filters and emerges as two signals; approximation and detailed (see Fig. 7), which are the high-scale (low-frequency) and the low-scale (high-frequency) components of the signal, respectively. Although the two-dimensional wavelet was used in the filtering process, the one-dimensional form of the wavelet equations is explained here (see Eqs.(3)–(7)) to simplify the expressions, since the implementation of two-dimensional wavelet transform is based on the one-dimensional wavelet transform in two directions. For more information on the two-dimensional wavelet transform, *Mallat (1998)* and *Elhabiby (2007)* can be consulted.

In DWT, the one-dimensional signal q is expressed using wavelet base functions as follows:

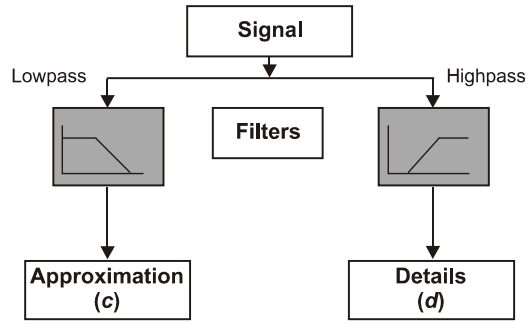

Fig. 7. Low and high pass wavelet filtering process at its most basic level (*Elhabiby, 2007*).

$$q(x) = q_c(x) + q_d(x) = \sum_{t \in Z} c_t^s \phi_{s,t}(x) + \sum_{s \in Z} \sum_{t \in Z} d_t^s \psi_{s,t}(x), \tag{3}$$

where $q_c(x)$ and $q_d(x)$ are the approximation and the detailed parts of the signal, c_t^s and d_t^s are the approximation and detailing coefficients, $\phi_{s,t}$ is the scaling function generated from the original form of the scaling function ϕ, $\psi_{s,t}$ is the wavelet function generated from the original mother wavelet function $\psi \in L^2(\Re)$, s is the scale (level) of decomposition and t is the shifting (translation) integer (*Mallat, 1998*). Then the approximation coefficients are given by

$$c_t^s = \langle q(x), \phi_{s,t} \rangle = \sum_t q(x) \phi_{s,t}(x). \tag{4a}$$

The scaling function in Eq.(4a) is represented by a number of lowpass filter coefficients a_t as

$$\phi_{s,t}(x) = \sqrt{2} \sum_{t \in Z} a_t \phi(2x - t) \tag{4b}$$

and thus the approximation part of the signal is given by

$$q_c(x) = \sum_{t \in Z} c_t^s \phi_{s,t}(x). \tag{5}$$

The detailing coefficients are derived from

$$d_t^s = \langle q(x), \psi_{s,t} \rangle = \sum_t q(x) \psi_{s,t}(x), \tag{6a}$$

where the wavelet function is represented by

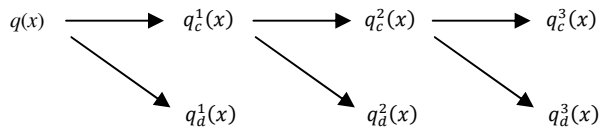

Fig. 8. The levels of decomposition in wavelet multi-resolution analysis.

$$\psi_{s,t}(x) = \sqrt{2} \sum_{t \in Z} g_t \phi(2x - t). \tag{6b}$$

In Eq.(6b), g_t are the highpass filter coefficients, and thus the detailed part of the signal is calculated with the following equation:

$$q_d(x) = \sum_{s \in Z} \sum_{t \in Z} d_t^s \psi_{s,t}(x). \tag{7}$$

As it is seen in Eq.(3), multiresolution analysis consists of splitting the signal $q(x)$ into lower and higher frequency components, $q_c(x)$ and $q_d(x)$, by application respectively of low pass and high pass filters (see Fig. 7), and recursively repeating this to the output of the low frequency filter (this is explained briefly by Eq.(8) and in Fig. 8). After J steps, the output consist of a series of high frequency sub-bands, $q_d^j(x)$, $j = 1, \ldots, J$, containing the detail of the signal at different resolutions, and the last low frequency sub-band, $q_c^j(x)$, containing a smooth approximation of the signal at the lowest resolution level considered, J.

$$\begin{aligned} q(x) &= g_c^1(x) + g_d^1(x) \\ &= g_c^2(x) + g_d^2(x) + g_d^1(x) \\ &= g_c^3(x) + g_d^3(x) + g_d^2(x) + g_d^1(x) = \ldots \end{aligned} \tag{8}$$

In this study, the appropriate resolution level of the decomposition was determined by trials. Different levels of decomposition were applied and the results were compared. As an example, the decomposition of the fifth and the sixth level DMWT of GPS/levelling data are compared in Fig. 9 and it can be seen that the fifth level of decomposition of the data (LPF(DMWT5)\GPS/Lev.) fits the GGM (EIGEN-CG03C) better than the sixth level (LPF(DMWT6)\GPS/Lev.). Fig. 10 shows the GPS/levelling data before and after filtering.

3.2. Testing GGMs Using Terrestrial Data

The GGM-derived gravity anomalies Δg_{GGM} were compared with the mean free-air gravity anomalies Δg_{FA} over the entire region of Turkey (Eq.(9)), and the GGM-derived geoid heights N_{GGM} were compared with the low-pass filtered GPS/levelling data $q_c(N_{GPS/lev})$ only in local areas (Eq.(10)).

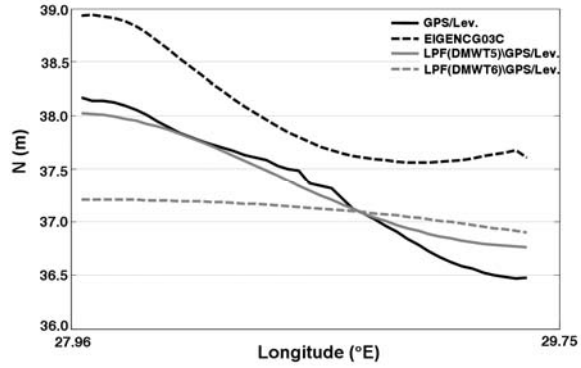

Fig. 9. GPS/levelling (before and after low-pass filtering with the fifth and sixth level of DMWT), and EIGENCG03C derived geoid heights at the benchmarks in Istanbul.

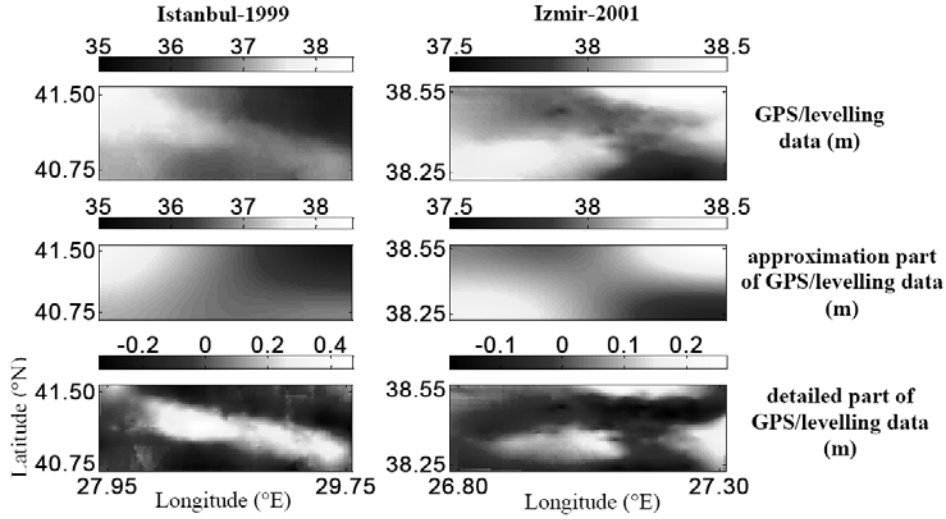

Fig. 10. Plots are the GPS/levelling geoid heights, their low-pass filtered (approximation) and the high-pass filtered (detailed) parts after DMWT of Istanbul-1999 and Izmir-2001 data, respectively.

$$d\Delta g = \Delta g_{FA} - \Delta g_{GGM} \,, \tag{9}$$

$$dN_{(1)} = q_c \left(N_{GPS/lev} \right) - N_{GGM} \,. \tag{10}$$

Here the GGMs were considered with their maximum expansions, since the purpose of the assessments was to test and compare the fit of the GGMs using their complete set of coefficients. Therefore the gravity anomalies and the geoid heights derived from each

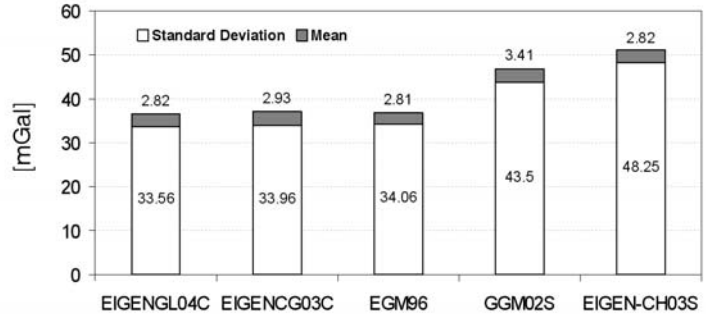

Fig. 11. Standard deviations and mean values of the residuals between the GGM-derived and free-air gravity anomalies over Turkey.

GGM were evaluated against the terrestrial data (instead of directly comparing the models with each other). Results of analysis on various truncations of the spherical harmonic coefficient sets can be found in *Merry (2007)*.

The statistical comparison of the GGM-derived and free-air gravity anomalies at grid nodes on land (in 30′ spatial resolution) is shown in Fig. 11. EGM96, EIGEN-CG03C and EIGEN-GL04C models show the best statistical fit to the free-air gravity anomalies over Turkey.

The statistical comparison between the GGM-derived geoid heights and the geometrically derived (low-pass filtered) geoid heights at the GPS/levelling benchmarks in local networks are shown in Table 4.

Fig. 12 illustrates the standard deviations of the geoid height differences between the GGM-derived and the filtered GPS/levelling data in Istanbul and Izmir networks.

Table 4. Statistics of the geoid height differences between GGM-derived and low-pass filtered GPS/levelling data in Istanbul-1999 and Izmir-2001 (units in cm).

GGM	ℓ_{max}	Min	Max	Mean	Std.Dev.
Istanbul-1999 Network					
GGM02S	110	−122.6	116.1	49.4	42.7
EIGEN-CH03S	60	−96.0	75.5	−40.8	29.1
EGM96	360	−154.0	−60.7	−106.2	27.0
EIGENCG03C	360	−152.4	−15.6	−81.8	41.4
EIGENGL04C	360	−151.3	21.1	−54.3	51.1
Izmir-2001 Network					
GGM02S	110	−82.0	−18.2	−44.5	11.5
EIGEN-CH03S	60	−323.6	−222.1	−267.9	21.0
EGM96	360	−204.6	−82.8	−141.1	25.8
EIGENCG03C	360	−139.6	−34.2	−83.6	21.3
EIGENGL04C	360	−149.7	−31.4	−89.6	25.2

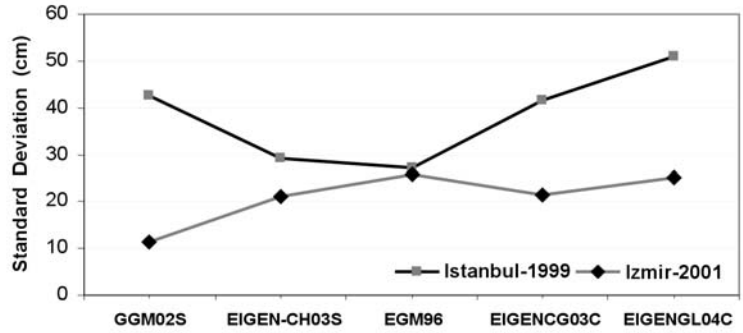

Fig. 12. Standard deviations of the geoid height differences between the GGM-derived and filtered GPS/levelling in Istanbul and Izmir.

The low-pass filtered GPS/levelling data provided an independent control for the GGMs in the local areas and made it possible to test the fit of the GGM to the local gravity field. In comparison to the other combined GGMs, EGM96 is more consistent in terms of accuracy in western Turkey. The standard deviations of the geoid height differences between the EGM96-derived and the filtered GPS/levelling data is around 25 cm both in Istanbul and Izmir. On the other hand, the EIGEN-CG03C has a better fit than EGM96 in Izmir, however it is worst than EGM96 in Istanbul.

3.3. Assessment of GGMs in Gravimetric Geoid Determination

In the second approach, gravimetric geoid models were computed using the RCR technique, where the complete expansions of the GGMs were employed in conjunction with the regional terrestrial gravity data via the unmodified spherical Stokes integral. Fig. 13 shows how the RCR technique was used in numerical tests and gives the basic steps of the applied approach. In each computed geoid model, a different GGM was used to remove and then restore the long-wavelength component of the gravity field, and the derived geoid heights were compared with the GPS/levelling heights at the benchmarks of the local networks.

The RCR technique implies that the effect of the GGM and the effect of the topography with its compensation should be removed from the employed gravity anomalies for computing the geoid; the mathematical expressions follow. The reduced gravity anomaly is

$$\Delta g = \Delta g_{FA} - \Delta g_{GGM} - \Delta g_H \tag{11}$$

and the computed geoid height is

$$N_{Grav} = N_{GGM} + N_{\Delta g} + N_{ind}\,, \tag{12}$$

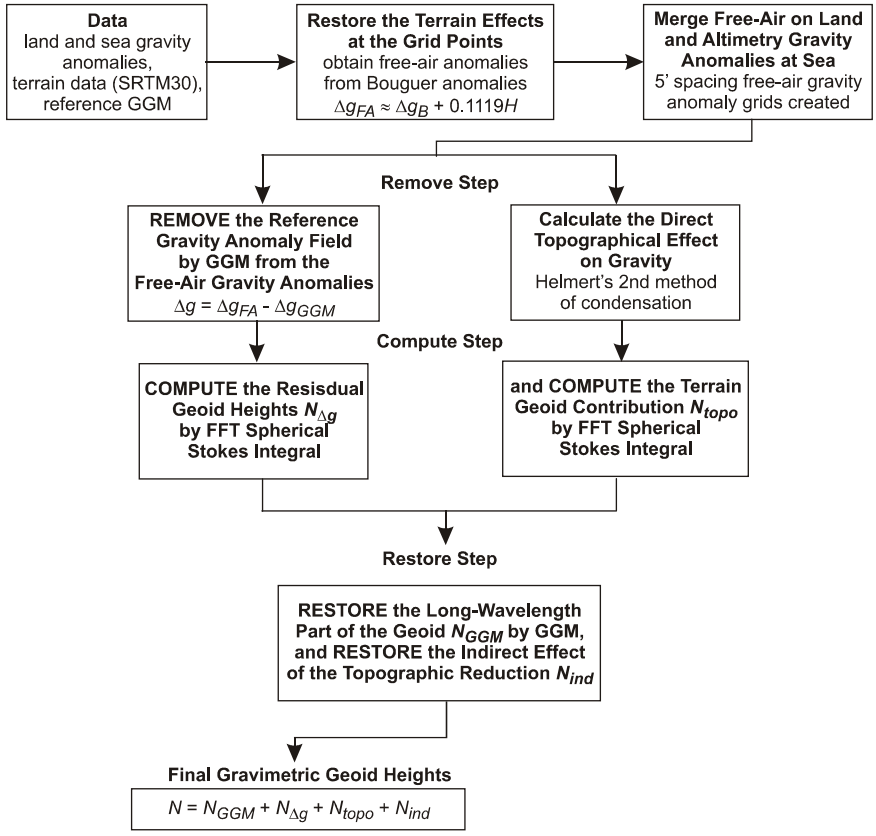

Fig. 13. The steps of the RCR technique as applied in gravimetric modelling of the geoids (*Erol, 2007*).

where Δg_{GGM} is the effect of the GGM on gravity anomalies, Δg_H is the terrain effect on gravity, N_{GGM} is the contribution of the GGM (expressed by the equation 1), $N_{\Delta g}$ is the residual geoid height, which is calculated using Stokes integral (see Eq.(13)) and N_{ind} is the indirect effect of the terrain on the geoid heights (see Eq.(17)) (*Heiskanen and Moritz, 1967*). The residual geoid height is computed from Stokes's equation

$$N_{\Delta g} = \frac{R}{4\pi\gamma} \iint_{\sigma} \Delta g S(\Psi)\, d\sigma\,, \tag{13}$$

where σ denotes the Earth's surface, Δg is the reduced gravity anomaly (see Eq.(11)) and $S(\Psi)$ is the Stokes kernel function

$$S(\Psi)=\frac{1}{\sin\frac{\Psi}{2}}-4-6\sin\frac{\Psi}{2}+10\sin^2\frac{\Psi}{2}+\left(3-6\sin^2\frac{\Psi}{2}\right)\ln\left(\sin\frac{\Psi}{2}+\sin^2\frac{\Psi}{2}\right), \quad (14)$$

where $\sin(\Psi/2)$ is expressed as

$$\sin^2\frac{\Psi}{2}=\sin^2\frac{\varphi_P-\varphi_Q}{2}+\sin^2\frac{\lambda_P-\lambda_Q}{2}\cos\varphi_P\cos\varphi_Q\,, \quad (15)$$

where Ψ is the spherical distance between the computation point $P(\varphi, \lambda)$ and the running point $Q(\varphi, \lambda)$ (*Haagmans et al., 1993*; *Sideris, 1994*). The 1D Fast Fourier Transform (FFT) technique was used for evaluating the convolution integrals using gridded data.

In Fig. 13, Δg_B are Bouguer gravity anomalies (with standard density $\rho = 2.67$ g/cm^3). The correction for the attraction of the Bouguer plate, $2\pi G\rho H$, was approximated by $0.1119\,H$, where H is the height in metres interpolated from the ETOPO5 digital elevation model. The free-air anomalies were obtained using the original Bouguer gravity anomaly data set. A grid of reduced free-air anomalies Δg was obtained and used to produce the residual geoid heights $N_{\Delta g}$. The terrain effects on gravity C (see Eq.(16)) were computed using the grid of SRTM data, and then the effect of the terrain corrections on the geoid heights N_{topo} were computed using the 2D Fast Fourier Transform technique. The GGM-derived geoid heights N_{GGM} were computed and restored in the Restore Step. The indirect effect (up to second order term) on the geoid N_{ind} was evaluated using SRTM data. Finally, the summation of the individual components (N_{GGM}, $N_{\Delta g}$, N_{topo}, N_{ind}) gave the gravimetric geoid heights N.

Helmert's second method of condensation was applied in gravity reduction. The terrain effect on gravity and the indirect effect on the geoid heights for Helmert's second method of condensation are given by Eqs.(16) and (17), respectively (*Heiskanen and Moritz, 1967*; *Sideris, 1994*):

$$C=-\Delta g_H=\frac{G\rho R^2}{2}\iint_\sigma\frac{\left(H_Q-H_P\right)^2}{S^3}\,d\sigma\,, \quad (16)$$

$$N_{ind}=-\frac{\pi G\rho H_P^2}{\gamma}-\frac{G\rho R^2}{6\gamma}\iint_\sigma\frac{H_Q^3-H_P^3}{S^3}\,d\sigma\,, \quad (17)$$

where G is the gravitational constant, ρ is the topographic density, and H_P and H_Q are the heights of the computation and running points, respectively. S is the planar distance between the points P and Q. Eqs.(16) and (17) were evaluated using the 2D FFT approach (*Li, 1993*; *Sideris, 1994*).

The practical implementation of the RCR technique involves certain approximations on evaluation of the topographic, atmospheric and ellipsoidal effects, which are discussed in, e.g., *Sjöberg (2005)* and should be considered to achieve a 1-cm geoid model. The investigation on the magnitudes of the adopted approximations in computing the regional geoid model is left to a future research and will not be considered in this investigation.

The computation steps as described above were carried using each GGM as the base model and thus five new gravimetric geoid models were calculated. For the assessments of precision of the models, they were fitted to the GPS/levelling surface (local vertical datum) using a third order polynomial model and thus de-trended. *Erol et al. (2008)* provides details on the selection process of model fitting. The final models were cross-validated considering the geoid height discrepancies $dN_{(2)}$ (Eq.(18)) between the fitted models and GPS/leveling - at the independent test benchmarks having homogeneous distribution in the area. The standard deviation of the final geoid model ($\sigma_{N_{model}}$) was considered as the absolute accuracy measure. The standard deviations of the discrepancies ($\sigma_{dN_{(2)}} \approx 5.5\,\text{cm}$ from the Table 5), ellipsoidal heights ($\sigma_H \approx 2.3\,\text{cm}$, see data description in Table 2) and orthometric heights ($\sigma_H \approx 2.3\,\text{cm}$, see Table 2) were employed to derive the standard deviation of the final model ($\sigma_{N_{model}} \approx \sqrt{\sigma^2_{dN_{(2)}} - \sigma^2_h - \sigma^2_H}$) considering Eq.(18) under the assumption that all systematic errors are removed by fitting and there are no correlations between h, H and N_{model}). The accuracy of the final models was also compared with TG03. $dN_{(3)}$ in equation 19 are the differences of TG03 (N_{TG03}) from the GPS/levelling undulations ($N_{GPS/lev}$).The absolute accuracy of TG03 ($\sigma_{N_{TG03}} \approx \sqrt{\sigma^2_{dN_{(3)}} - \sigma^2_h - \sigma^2_H}$) was calculated employing the standard deviations of geoid height differences ($\sigma_{dN_{(3)}} \approx 9\,\text{cm}$), ellipsoidal (σ_h) and orthometric (σ_H) heights

$$dN_{(2)} = N_{GPS/lev} - N_{model} = h - H - N_{model}\,, \tag{18}$$

$$dN_{(3)} = N_{GPS/lev} - N_{TG03} = h - H - N_{TG03}\,. \tag{19}$$

The statistics of the assessments of new models against GPS/levelling data are in Table 5. Fig. 14 compares the accuracies of the new models and TG03.

The conclusions drawn from the numerical results are the following:

a) When the geoid heights derived from the models are compared with GPS/levelling at the test benchmarks, the absolute accuracies of the new geoid models with fitting are calculated around 4.9 cm, which satisfies the criterion for deriving orthometric heights from GPS ellipsoidal heights for geodetic purposes using a geoid model given in the Large Scale Map and Spatial Data Production Regulation of Turkey (*Deniz et al., 2008*). Thus, any of these models can be recommended to be used for vertical control in geodetic applications in Istanbul and Izmir territories.
b) When the gravimetric geoid was computed only from a GGM, results showed that EGM96 and EIGEN-CHAMP03S performed the best and they are therefore recommended to derive the long wavelength part of the gravity field in the region (see Table 4, Fig. 12). As expected, all the test models revealed similar performances in gravimetric geoid modelling using the RCR approach (see Tables 5a and 5b), thus illustrating the importance of local gravity and topography data.

Table 5. Statistics of the geoid height differences ($dN_{(2)}$) in Istanbul-1999 and Izmir-2001 networks (in cm).

Model No	Reference GGM	Statistics*	Min	Max	Mean	Std.Dev.
Istanbul-1999 Network						
I	GGM02S (ℓ_{max} = 110)	Internal	−18.8	32.8	0.0	5.7
		External	−19.3	33.7	0.0	5.9
II	EIGEN CHAMP03S (ℓ_{max} = 60)	Internal	−18.6	33.7	0.0	5.6
		External	−19.1	34.7	0.0	5.9
III	EGM96 (ℓ_{max} = 360)	Internal	−18.6	34.6	0.0	5.6
		External	−19.1	35.6	0.0	5.8
IV	EIGENCG03C (ℓ_{max} = 360)	Internal	−18.2	34.2	0.0	5.9
		External	−19.2	35.3	0.0	6.1
V	EIGENGL04C (ℓ_{max} = 360)	Internal	−17.3	33.2	0.0	5.5
		External	−17.8	34.1	0.0	5.8
Izmir-2001 Network						
I	GGM02S (ℓ_{max} = 110)	Internal	−14.3	16.1	0.0	5.3
		External	−15.0	16.4	0.0	5.5
II	EIGEN CHAMP03S (ℓ_{max} = 60)	Internal	−15.3	15.5	0.0	5.8
		External	−17.1	17.2	0.0	6.0
III	EGM96 (ℓ_{max} = 360)	Internal	−17.2	14.0	0.0	5.7
		External	−18.0	14.3	0.0	5.9
IV	EIGENCG03C (ℓ_{max} = 360)	Internal	−16.4	14.0	0.0	5.5
		External	−17.2	14.3	0.0	5.7
V	EIGENGL04C (ℓ_{max} = 360)	Internal	−15.3	13.5	0.0	5.8
		External	−15.9	14.2	0.0	6.0

* **Internal statistics:** the statistics of the geoid height differences at the GPS/levelling benchmarks used in the determination of the parametric model (the third order polynomial) for fitting gravimetric geoid model to the regional vertical datum. **External statistics:** the statistics of the cross-validation tests carried out considering geoid height discrepancies at independent test benchmarks distributed homogeneously on the area (for further explanations on determining the fitting surface model and cross-validation test, *Erol et al. (2008)* can be consulted).

c) The new models provided an improved accuracy compared to TG03 (the absolute accuracy of the new geoid models $\sigma_{N_{model}}$ is around 4.9 cm whereas the absolute accuracy of TG03 model $\sigma_{N_{TG03}}$ is 8.4 cm) (see Figure 14). This is because of the improved density and quality of the terrestrial gravity and GPS/levelling data that were employed in calculating and fitting the new models to the regional datum, respectively. This result emphasizes the role of quality of high-frequency information for precise local geoid modelling.

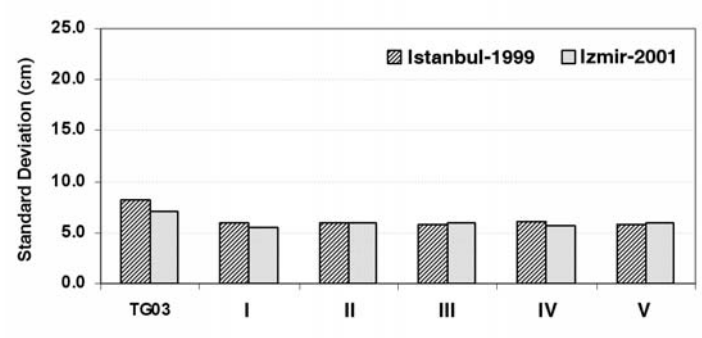

Fig. 14. Standard deviations of the geoid height differences of the TG03 ($dN_{(3)}$), and of the fitted gravimetric geoid models ($dN_{(2)}$) from the GPS/levelling.

4. CONCLUSIONS

Recent GGMs from the CHAMP and GRACE missions were evaluated using external ground-truth data in Turkey. A series of numerical tests were carried out using GGMs, terrestrial gravity and topography data, local GPS/levelling data (with and without filtering) and TG03 geoid data. The conclusions drawn after detailed evaluations are as follows.

- A high degree combined GGM (EIGEN-CG03C, EIGEN-GL04C and EGM96 with $\ell_{max} = 360$) fits the terrestrial gravity data better compared to the satellite-only GGMs (EIGEN CHAMP03S and GGM02S with $\ell_{max} = 60$ and $\ell_{max} = 110$, respectively), and the combined models are recommended for use in determining the gravity anomalies over Turkey. This result is (self)evident from a theoretical point of view, as the pure satellite GGMs determine only low-degrees, while terrestrial gravity data is mainly at high degrees.

  When testing the GGMs against independent gravity field and geoid information, the filter used for smoothing the control data, the omission/commission errors and the impact of the long-wavelengths introduce some problems that must be treated carefully.
- Here, the (fifth level) DMWT method was applied to filter the local GPS/levelling data, but various other models could also be used to filter these data. The comparisons of the geoid values from GGMs with the approximation component of the wavelet-filtered GPS/levelling heights showed that the EGM96 model is good in representing the long-wavelength geoid in western Turkey. Similar analyses were done and the same conclusion on EGM96 was drawn by *Kiamehr and Sjöberg (2005)*, *Rodriguez-Caderot et al. (2006)* and *Merry (2007)*, in Iran, Southern Spain and Southern Africa, respectively. In western Turkey, the standard deviation of the differences between EGM96 and GPS/leveling-derived geoid heights is 26 cm. EIGEN-CHAMP03S also compares very well, with a standard deviation of 25 cm for the geoid height differences.

- GGM02S fits the filtered GPS/levelling undulations the best in Izmir (with a standard deviation of 11 cm), but the worst in Istanbul (with a standard deviation of 43 cm). The EIGENCG03C and EIGENGL04C models yielded 24 cm and 45 cm in standard deviation of the geoid height differences when they were compared with GPS/levelling undulations in the Izmir and Istanbul local areas, respectively. Thus EGM96 and EIGEN-CHAMP03S are suggested for representing the long-wavelength geoid in the West of Turkey.

  As part of the continuous efforts since the 1970's to determine a precise and detailed geoid for Turkey, gravimetric test geoids were calculated using local data with each GGM in western Turkey, and were compared using independent GPS/levelling undulations. The outcomes of these efforts showed that:
- Any of the tested GGMs can be employed as the reference model for calculating the high-resolution gravimetric geoid model but only if the model is used after fitting it to the regional vertical datum through the available GPS benchmarks.
- The new geoid models with fitting to the regional vertical datum have a 4.9 cm absolute accuracy, and are recommended to be used for geodetic vertical control purposes.

The new geoid models provided 42% improvement in absolute accuracy compared to the TG03 model. This improvement is most likely due to the dense and high-quality terrestrial gravity, GPS/levelling and topography data that were used in computing and fitting the gravimetric test geoids; the difference between the densities of the GPS/levelling benchmarks used for fitting to the regional datum the new test geoids and TG03 is obvious from the Figs. 3 and 4. It is recommended that the density and accuracy of the terrestrial gravity and GPS/levelling data that will be employed to compute future national geoid models in Turkey should be improved. In addition, a computation methodology that optimally combines heterogeneous data, with particular emphasis on the modelling of systematic errors and datum inconsistencies and propagation of random errors, should be employed.

Acknowledgements: The first author was supported by a research grant from the Scientific and Technological Research Council of Turkey (TUBITAK) during this study. Prof. J.D. Fearhead and GETECH Ltd. at the University of Leeds are acknowledged for providing Bouguer gravity anomalies and Prof. Dr. A. Ateş from Ankara University is gratefully acknowledged for providing gravity information for this research.

References

Ayan T., 1976. *Astrogeodätische Geoidberechnung für das Gebiet der Türkei*. PhD Thesis, Karlsruhe University, Karlsruhe, Germany (in German).

Ayan T., Aksoy A., Deniz R., Arslan E., Çelik R.N., Özşamlı C., Denli H.H., Erol S. and Erol B., 1999. *Istanbul GPS Triangulation Network (İGNA) Project*. ITU Report No. ITU 1997/3882, Istanbul Technical University, Istanbul, Turkey (in Turkish).

Ayan T., Deniz R., Çelik R.N., Denli H., Ozludemir T., Erol S., Erol B., Akyilmaz, O. and Guney C., 2001. *Izmir Geodetic Reference System–2001*. ITU Report No. ITU 2000/2294, Istanbul Technical University, Istanbul, Turkey (in Turkish).

Ayhan M.E., 1993. Geoid determination in Turkey. *Bulletin Geodesique*, **67**, 10–22.

Ayhan M.E. and Kılıçoğlu, A., 1993. Turkey Doppler geoid (TDG). *Prof. Dr. H. Wolf Geodesy Symposium*, Chamber of Turkish Surveying Engineers, Istanbul, Turkey, 409–435.

Deniz R., Çelik R.N., Kutoğlu H., Özlüdemir M.T., Demir C. and Kınık İ., 2008. Large scale map and spatial data production regulation. In: Deniz R. and Çelik R.N. (Eds.), *Inc: bylaw legalized in July 2005*. Chamber of Turkish Surveying Engineers, Istanbul, Turkey, 31–42. (http://www.hkmo.org.tr/resimler/ekler/2CO1_db11d259a9db7fb_ek.pdf, in Turkish).

EGM96, 2004. *NASA Goddard Space Flight Center (GSFC) and NIMA Joint Geopotential.* http://cddis.nasa.gov/926/egm96/egm96.html.

Elhabiby M.M., 2007. *Wavelet Representation of Geodetic Operators*. PhD Thesis, UCGE Reports (20250), University of Calgary, Faculty of Graduate Studies, Calgary, Canada.

Erol B., 2007. *An Investigation on Local Geoids for Geodetic and Surveying Applications*. PhD Thesis, Istanbul Technical University, Istanbul, Turkey.

Erol B., Erol S. and Çelik R.N., 2008. Height transformation using regional geoids and GPS/levelling in Turkey. *Survey Review*, **40(307)**, 2–18.

EROS, 2002. *Earth Resources Observation and Science (EROS) Website*. Data Center, U.S. Geological Survey, (http://edc.usgs.gov/).

Farr T.G. and Kobrick M., 2000. Shuttle radar topography mission produces a wealth of data. *EOS Trans. AGU*, **81**, 583–585.

Förste C., Flechtner F., Schmidt R., Meyer U., Stubenvoll R., Barthelmes F., Rothacher M., Biancale R., Bruinsma S. and Lemoine J.M., 2005. A new high resolution global gravity field model from the combination of GRACE satellite mission and altimetry/gravimetry surface gravity data. *Geophys. Res. Abstracts*, **7**, 04561.

Förste C., Flechtner F., Schmidt R., König R., Meyer U., Stubenvoll R., Rothacher M., Barthelmes F., Neumayer H., Biancale R., Bruinsma S., Lemoine J.M. and Loyer S., 2006. A Mean Global Gravity Field Model from the combination of satellite mission and altimetry/gravimetry surface data. *Geophys. Res. Abstracts*, **8**, 03462.

Förste C., Schmidt R., Stubenvoll R., Flechtner F., Meyer U., König R., Neumayer H., Biancale R., Lemoine J.M., Bruinsma S., Loyer S., Franz B. and Esselborn S., 2008. The GeoForschungsZentrum Potsdam/Groupe de Recherche de Gèodésie Spatiale satellite-only and combined gravity field models: EIGEN-GL04S1 and EIGEN-GL04C. *J. Geodesy*, **82**, 331-346, doi: 10.1007/s00190-007-0183-8.

GFZ, 2006. *The CHAMP Mission, Germany.* (http://www.gfz-potsdam.de/pb1/op/champ /results/grav/010_eigen-champ03s.html).

GGM02, 2004. *GRACE Gravity Model 02*. Center of Space Research (CSR) of the University of Texas at Austin, Austin, Texas, U.S. (http://www.csr.utexas.edu/grace/gravity/).

Gruber T., 2004. Validation concepts for gravity field models from new satellite missions. (http://earth.esa.int/workshops/goce04/participants/).

Haagmans R., de Min E. and van Gelderen M., 1993. Fast evaluation of convolution integrals on the sphere using 1D FFT and a comparison with existing methods for Stokes integral. *Manuscripta Geodaetica*, **18**, 227–241.

Heiskanen W.A. and Moritz H., 1967. *Physical Geodesy*. WH Freeman, San Francisco.

ICGEM, 2005. *Table of Available Models*. International Center for Global Earth Models, GeoForschungsZentrum Potsdam (GFZ), Germany (http://icgem.gfz-potsdam.de /ICGEM/ICGEM.html).

Kiamehr R. and Sjöberg L.E., 2005. Comparison of the qualities of recent global and local gravimetric geoid models in Iran. *Stud. Geophys. Geod.,* **49**, 289–304.

KMS, 2002. *Global Marine Free-Air Gravity Field-KMS2002 - March 2003*. The Danish National Space Center, Copenhagen, Denmark (http://geodesy.spacecenter.dk/GRAVITY/).

Lemoine F.G., Kenyon S.C., Factor J.K., Trimmer R.G., Pavlis N.K., Chinn D.S., Cox C.M., Klosko S.M., Luthcke S.B., Torrence M.H., Wang Y.M., Williamson R.G., Pavlis E.C., Rapp R.H. and Olson T.R., 1998. *The Development of the Joint NASE GSFC and the National Imagery and Mapping Agency (NIMA) Geopotential Model EGM96*. NASA Technical Report NASA/TP-1996/8-206861, NASA, Greenbelt, Maryland, USA.

Li Y.C., 1993. *Optimized Spectral Geoid Determination*. MSc Thesis, Department of Geomatics Engineering, University of Calgary, Calgary, Canada.

Mallat S., 1998. *A Wavelet Tour of Signal Processing.* Academic Press, New York.

Merry C.L., 2007. Evaluation of global geopotential models in determining the quasi-geoid for Southern Africa. *Surv. Rev.*, **39**, 180–192.

NIMA, 1997. *World Geodetic System 1984. NIMA TR8350.2, The Third Edition*, National Imagery and Mapping Agency, Department of Defense, U.S.

NOAA, 2005. *ETOPO5 Data and Documentation Website*. National Geophysical Data Center (NGDC), National Oceanic and Atmospheric Administration (NOAA) Satellite and Information Service, U.S. (http://www.ngdc.noaa.gov/mgg/fliers/ 93mgg01.html).

Reigber Ch., Jochmann H., Wünsch J., Petrovic S., Schwintzer P., Barthelmes F., Neumayer K.-H., König R., Förste Ch., Balmino G., Biancale R., Lemoine J.-M., Loyer S. and Perosanz F., 2004. Earth gravity field and seasonal variability from CHAMP. In: Reigber Ch., Lühr H., Schwintzer P. and Wickert J. (Eds.), *Earth Observation with CHAMP - Results from Three Years in Orbit*, Springer-Verlag, Berlin, 25–30.

Rodriguez-Caderot G., Lacy M.C., Gil A.J. and Blazquez B., 2006. Comparing recent geopotential models in Andalusia (Southern Spain). *Stud. Geophys. Geod.*, **50**, 619–631.

Rummel R., Balmino G., Johannessen J., Visser P. and Woodworth P., 2002. Dedicated gravity field missions–principles and aims. *J. Geodyn.*, **33**, 3–20.

Sideris M.G., 1994. *Geoid Determination by FFT Techniques*. Lecture Notes - International School for the Determination and Use of the Geoid. International Geoid Service, DIIAR - Politecnico di Milano, Italy, 213–272.

Sjöberg L.E., 2005. A discussion on the approximations made in the practical implementation of the remove-compute-restore technique in regional geoid modelling. *J. Geodesy*, **78**, 645–653.

Smith D.A., 1998. There is no such thing as "The" EGM96 geoid: Subtle points on the use of a global geopotential model. *IGeS Bulletin*, **8**, 17–28.

SRTM, 2000. *Shuttle Radar Topography Mission*, NASA Jet Propulsion Laboratory (http://www2.jpl.nasa.gov/srtm/).

Tapley B., Ries J., Bettadpur S., Chambers M., Cheng M., Condi F., Gunter B., Kang Z., Nagel P., Pastor R., Pekker T., Poole S. and Wang F., 2005. GGM02 - an improved Earth gravity field model from GRACE. *J. Geodesy*, **79**, 467–478.

TNFGN, 2002. Turkish national fundamental GPS network - 1999. *General Command of Mapping, Map Journal Special Edition*, **16**, 27–31 (in Turkish).

TNGC, 2003. *Report of Turkish National Geodesy Commission for the period of 1999–2003.* International Union of Geodesy and Geophysics (IUGG), Sapparo, Japan, 4–26 (http://www.iugg.org/members/nationalreports/turkey.pdf).

UCSD, 2005. *Satellite Geodesy.* Scripps Institution of Oceanography, University of California, La Jolla, California, U.S. (http://topex.ucsd.edu/).